Table 1 Doping dependence of the strong coupling ratio

Doping level	Arpes*	Tunnelling	Andreev reflection	$\lambda(T)$	Raman scattering
Optimally doped					
BSCCO	9 (ref. 3)	5 (refs 4, 15)		6 (ref. 20)	6 (ref. 22)
YBCO		8 (ref. 11)	5 (ref. 12)	5 (ref. 20)	
LSCO		7.5 (refs 17, 18)	5 (ref. 17)		5 (ref. 25)
$HgBa_2CaCu_2O_{6+\delta}$					5 (ref. 26)
Overdoped					
BSCCO (60 K)		6–9 (refs 4, 15)			6 (ref. 22)
Underdoped					
BSCCO (80 K)	11–13 (ref. 27)	12 (refs 4, 15)	6.2 (ref. 16)		
BSCCO (70 K)		14 (ref. 15)			5 (ref. 22)
YBCO (60–65 K)		20 (ref. 3)	4.6 (ref. 14)	5 (ref. 21) 4 (ref. 20)	
LSCO (15 K)			4.5 (ref. 17)		

The values of the strong coupling ratio ($2\Delta/kT_c$) shown here were obtained using the indicated methods of gap measurement (see text for details). The strong coupling ratio ranges from 6 to 20 for Δ_p (ARPES, tunnelling), and from 4 to 6 for Δ_c (Andreev reflection, $\lambda(T)$, Raman scattering).
* Angle-resolved photoemission spectroscopy.

values have been obtained by surface-sensitive measurements, while Δ_c values have been obtained from both surface (Andreev) and bulk measurements ($\lambda(T)$ and Raman), and may therefore be more reliable. Yet the persistence of Δ_p above T_c in the underdoped regime is in good agreement with a decrease of the spin susceptibility below a temperature $T^* > T_c$, which is a bulk measurement[1].

A related question is that of the mechanism leading to pair formation. A non-mean-field behaviour may just indicate the presence of strong phase fluctuations, and not necessarily the presence of preformed pairs in the Mott sense[23]. Both local pairs and the stripe model may explain the continuous increase of Δ_p in the underdoped regime. But if the existence of two energy scales was simply due to fluctuation effects, one would expect Δ_p to saturate in the underdoped regime[24]. It is also possible that Δ_p might be unrelated to a pairing amplitude.

In any case, I consider that the existence of two energy scales is well established in the underdoped regime, with the scales converging in the overdoped regime. I have assigned the lower scale, obtained from Andreev reflection experiments, to coherence properties of the condensate; the higher scale reflects the properties of single-particle excitations. □

Note added in proof: I have learned of theoretical work on the superfluid density and the excitation gap in a BCS–Bose–Einstein crossover scenario[28].

1. Alloul, H., Ohno, T. & Mendels, P. Y NMR evidence for a Fermi liquid behavior in $YBa_2Cu_3O_{6+x}$. *Phys. Rev. Lett.* **63**, 1700–1703 (1989).
2. Ding, H. *et al.* Spectroscopic evidence for a pseudogap in the normal state of underdoped high-T_c superconductors. *Nature* **382**, 51–54 (1996).
3. Racah, D. & Deutscher, G. Properties of normal metal/dielectric/high T_c junctions obtained by in-situ oxidation. *Physica C* **263**, 218–224 (1996).
4. Renner, C. *et al.* Pseudo-gap precursor of the superconducting gap in under- and overdoped $Bi_2Sr_2CaCu_2O_{8+\delta}$. *Phys. Rev. Lett.* **80**, 149–152 (1998).
5. Griffin, A., Snoke, D. W. & Stringari, S. (eds) *Bose-Einstein Condensation* (Cambridge Univ. Press, 1995).
6. Emery, V. J., Kivelson, S. A. & Zachar, O. Spin-gap proximity effect mechanism of high temperature superconductivity. *Phys. Rev. B* **56**, 6120–6147 (1997).
7. Deutscher, G. Superconducting glass and related properties. *Physica C* **153–155**, 15–20 (1988).
8. Pines, D. The spin fluctuation model for high temperature superconductivity: progress and prospects. In *The Gap Symmetry and Fluctuations in High Temperature Superconductors* (eds Bok, J., Deutscher, G., Pavuna, D. & Wolf, S.) (NATO ASI ser., Plenum, 1998).
9. Uemura, Y. J. Bose Einstein to BCS cross-over picture for high T_c cuprates. *Physica C* **282–287**, 194–197 (1997).
10. Zhao, G.-m., Hunt, M. B., Keller, H. & Müller, K. A. Evidence for polaronic supercarriers in the copper oxide superconductors $La_{2-x}Sr_xCuO_4$. *Nature* **385**, 236–239 (1996).
11. Maggio-Aprile, I. *et al.* Direct vortex imaging and tunneling spectroscopy of flux lines in $YBa_2Cu_3O_{7-\delta}$. *Phys. Rev. Lett.* **75**, 2754–2757 (1997).
12. Hass, N. *et al.* Sharp gap edge and determination of the Fermi velocity in $YBa_2Cu_3O_{7-\delta}$ by point contact spectroscopy. *J. Supercond.* **5**, 191–194 (1992).
13. Tanaka, Y. in *Coherence in High Temperature Superconductors* (eds Deutscher, G. & Revcolveschi, A.) 393–413 (World Scientific, Singapore, 1996).
14. Yagil, Y. *et al.* Experimental evidence for strong electron-phonon coupling to selected phonon modes in point contact spectroscopy. *Physica C* **250**, 59–66 (1995).
15. Miyakawa, N. *et al.* Strong dependence of the superconducting gap on oxygen doping from tunneling measurements on $Bi_2Sr_2CaCu_2O_{8-\delta}$. *Phys. Rev. Lett.* **80**, 157–160 (1998).
16. Sinha, S. & Ng, K. W. Zero bias conductance peak enhancement in $Bi_2Sr_2CaCu_2O_8$/Pb tunneling junctions. *Phys. Rev. Lett.* **80**, 1296–1299 (1998).
17. Achsaf, N. *et al.* in *Coherence in High Temperature Superconductors* (eds Deutscher, G. & Revcolveschi, A.) 428–442 (World Scientific, Singapore, 1996).
18. Ekino, T. *et al.* Superconducting energy gap of $La_{1.85}Sr_{0.15}CuO_4$ single crystals from breakjunction tunneling. *Physica C* **263**, 249–256 (1996).
19. Kohen, A. *Transition from s-wave to d-wave Gap Symmetry in $La_{2-x}Sr_xCuO_4$*. Thesis, Tel Aviv Univ. (1997).
20. Panapogoulos, C., Cooper, J. R. & Xiang, T. Systematic behavior of the in-plane penetration depth in d-wave superconductors. *Phys. Rev. B* **57**, 13422–13425 (1998).
21. Bonn, D. A. *et al.* Comparison of the influence of Ni and Zn impurities on the electromagnetic properties of $YBa_2Cu_3O_{6.95}$. *Phys. Rev. B* **50**, 4051–4063 (1995).
22. Nemetschek, R. *et al.* Pseudogap and superconducting gap in the electronic Raman spectra of underdoped cuprates. *Phys. Rev. Lett.* **78**, 4837–4840 (1997).
23. Mott, N. V. High temperature superconductors above T_c. *Physica A* **168**, 221–228 (1990).
24. Lee, P. A. & Wen, X. G. Unusual superconducting state of underdoped cuprates. *Phys. Rev. Lett.* **21**, 4111–4114 (1997).
25. Chen, X. K. *et al.* Investigation of the superconducting gap in $La_{2-x}Sr_xCuO_4$ by Raman scattering. *Phys. Rev. Lett.* **73**, 3290–3293 (1994).
26. Sacuto, A. *et al.* Nodes of the superconducting gap probed by electronic Raman scattering in $HgBa_2CaCu_2O_{6+\delta}$ *Europhys. Lett.* **39**, 207–210 (1997).
27. Harris, J. M. *et al.* Anomalous superconducting gap size versus T_c behavior in underdoped $Bi_2Sr_2Ca_{1-x}Dy_xCu_2O_{8+\delta}$. *Phys. Rev. B* **54**, 15665–15668 (1996).
28. Chen, Q. *et al. Phys. Rev. Lett.* **81**, 4708 (1998).

High-temperature weak ferromagnetism in a low-density free-electron gas

D. P. Young*, D. Hall*, M. E. Torelli*, Z. Fisk*†, J. L. Sarrao†, J. D. Thompson†, H.-R. Ott‡, S. B. Oseroff§, R. G. Goodrich‖ & R. Zysler¶

* NHMFL, Florida State University, Tallahassee, Florida 32306, USA
† Material Science and Technology Division, Los Alamos National Laboratory, Los Alamos, New Mexico 87454, USA
‡ Laboratorium für Festköperphysik, ETH-Hönggerberg, CH-8093 Zürich, Switzerland
§ Department of Physics, San Diego State University, San Diego, California 92182, USA
‖ Department of Physics, Louisiana State University, Baton Rouge, Louisiana 70803, USA
¶ Centro Atomico Bariloche, Bariloche RN 8400, Argentina

The magnetic properties of the ground state of a low-density free-electron gas in three dimensions have been the subject of theoretical speculation and controversy for seven decades[1]. Not only is this a difficult theoretical problem to solve, it is also a problem which has not hitherto been directly addressed experimentally. Here we report measurements on electron-doped calcium hexaboride (CaB_6) which, we argue, show that—at a density of 7×10^{19} electrons cm^{-3}— the ground state is ferromagnetically polarized with a saturation moment of $0.07\,\mu_B$ per electron. Surprisingly, the magnetic ordering temperature of this itinerant ferromagnet is 600 K, of the order of the Fermi temperature of the electron gas.

The cubic hexaborides of the rare-earth elements have long attracted interest because of their wide variety of physical properties in spite of their simple crystallographic structures. These physical properties include very low work functions leading to the use of LaB_6 as a thermionic emitter[2,3], dense Kondo behaviour and electric quadrupole ordering in CeB_6 (ref. 4), Kondo insulating properties in SmB_6 (ref. 5), and low-carrier-density ferromagnetism in the local moment system EuB_6 (refs 6, 7).

The host material for the present experiments is the divalent alkaline-earth hexaboride CaB_6. The crystal structure of this material
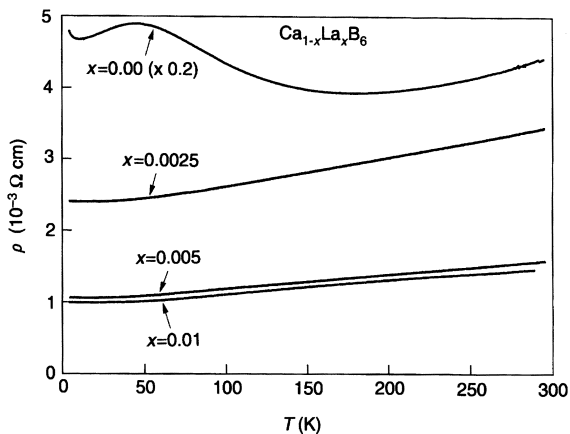
Figure 1 Temperature dependences of the electrical resistivities of La-doped CaB_6. The resistivity for pure CaB_6 has been multiplied by 0.2.
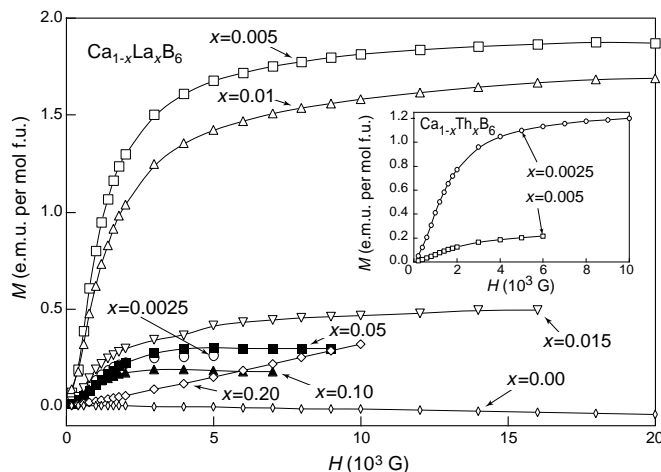

Figure 2 Magnetization per mol of compound versus applied field for La-doped CaB_6, measured at 5 K (f.u., formula unit). The data for $x = 0$ were taken at 10 K. Inset, magnetization versus applied field at 5 K for $Ca_{0.9975}Th_{0.0025}B_6$ and $Ca_{0.995}Th_{0.005}B_6$. Magnetizations have been measured after cooling in zero field, using a Quantum Design SQUID magnetometer.

can be thought of as a simple cubic CsCl-type arrangement of B_6-octahedra and metal ions. The early electronic structure cluster calculations of Longuet-Higgins and Roberts[8] found that the linked B_6-network required 20 electrons for a 'closed shell' electronic configuration, indicating that the alkaline-earth hexaborides would be semiconductors. A study of the low-temperature properties of single crystals of SrB_6, however, found a non-zero conductivity due to approximately 0.001 electrons per SrB_6, and indications of the importance of electron–hole Coulomb effects[9]. More recent band structure calculations[10] show that hexaborides with divalent cations should be semimetals, with a small direct overlap of a primarily boron-derived valence band with a primarily alkaline-earth-derived conduction band at the X-point in the Brillouin zone.

Our experiments, including measurements of the electrical resistivity, the magnetic susceptibility and the magnetization, were performed on single crystals of CaB_6 doped with trivalent La; these crystals were grown from stoichiometric amounts of the hexaboride components in molten Al. On similarly prepared single crystals of $Sr_{1-x}Ce_xB_6$, we have verified that Ce is incorporated stoichiometrically into the crystals by measuring the magnetic susceptibility and fitting the data to a Curie–Weiss law with an effective moment $\mu_{eff} = 2.54\,\mu_B$ per trivalent Ce ion. It is reasonable to assume that the neighbour of Ce in the rare-earth sequence, La, is also incorporated stoichiometrically in SrB_6 and CaB_6. X-ray diffraction has confirmed the cubic hexaboride structure in all cases.

Figure 1 shows the electrical resistivity data obtained between 5 K and 300 K from single crystals of $Ca_{1-x}La_xB_6$. Already for $x = 0.005$, we find a change to a metallic-like temperature dependence and a drop in resistivity by a factor of ~50 at low temperature, relative to the pure host ($x = 0$). A single band interpretation of the Hall constant obtained using the van der Pauw geometry for the $x = 0.005$ sample indicates electron-like carriers, with a density of 0.005 electrons per formula unit, as one naively expects for the trivalent La substitution. Our preliminary de Haas-van Alphen experiment on $x = 0.005$ La-doped CaB_6 along (100) reveals two orbits. Interpreting these as orthogonal extremal orbits of an ellipsoid gives an occupied volume (taking account of the ellipsoids at the equivalent X-points in the Brillouin zone) enclosing ~0.01 electrons for unpolarized electrons. This value is within experimental error of 0.005 electrons, given the small number of oscillations observed; the observation of two rather than four extremal orbits is consistent with the small hole pocket being filled, leaving only a small filling of the conduction band.

The unusual aspect of these La-doped borides is seen in Fig. 2, where we plot magnetization versus field at 5 K for a range of values of x, measured on single crystals of $Ca_{1-x}La_xB_6$. A weak ferromagnetic moment is evident, its magnitude peaking near $x = 0.005$ at $0.07\,\mu_B$ per La, with no moment found in crystals with composition $Ca_{0.80}La_{0.20}B_6$ (Fig. 3); hysteresis loops for the $x = 0.005$ material are shown in Fig. 3 inset. We find nearly identical magnetic effects with La-doping of CaB_6, SrB_6 and BaB_6. In all cases, the maximum moment is found at $x = 0.005$. That this moment is a function of the carrier concentration is supported by data for $Ca_{0.9975}Th_{0.0025}B_6$ and $Ca_{0.995}Th_{0.005}B_6$ (Fig. 2 inset): here the moment is maximum at $x = 0.0025$. Because Th is incorporated in a tetravalent configuration, it will contribute one more electron than trivalent La, and hence if the moment is a function of carrier count, compounds with $Th_{0.0025}$ and $La_{0.005}$ should have the same moment. In Fig. 4, we show the temperature dependence of the magnetic moment of $Ca_{0.995}La_{0.005}B_6$ in a fixed field of 0.1 T as a function of temperature: the data show loss of magnetization near the Curie temperature, T_C, of approximately 600 K.

The essential point is to determine that the observed weak ferromagnetism is an intrinsic effect and not of some extrinsic origin. The magnitude of the ordered moment is ~1 e.m.u. per mol hexaboride for $x = 0.005$ in CaB_6, and is ~2 e.m.u. per mol for $Sr_{0.995}La_{0.005}B_6$. We find consistently that the moment per mole is at a maximum near $x = 0.005$ in both SrB_6 and CaB_6. The same systematic study has not yet been made for BaB_6. We find similarly that Ce- and Sm-doped SrB_6 samples have an ordered moment which peaks at $x = 0.005$. In addition, however, we recognize the expected paramagnetic background due to the local magnetic moment due to the f-electrons of these atoms, which is absent for La-doped material. These data indicate that the doping does not produce the moment through trace rare-earth impurities carried by the high-purity La used for the doping. For the pure alkaline-earth hexaborides, we find that a moment is present sometimes, and that this varies from crystal to crystal. This moment is generally distinctly smaller than that found at $x = 0.005$, usually by at least an order of magnitude. We also find a variation in the temperature dependence of the electrical resistivity of pure SrB_6 and CaB_6 from crystal to crystal; crystals showing weak ferromagnetism have a more metallic temperature dependence of the electrical resistivity. Doping divalent hexaborides with other alkaline earths also produces weak ferromagnetism, for instance in $Ca_{0.995}Ba_{0.005}B_6$. We can understand this variable behaviour of the crystals with no
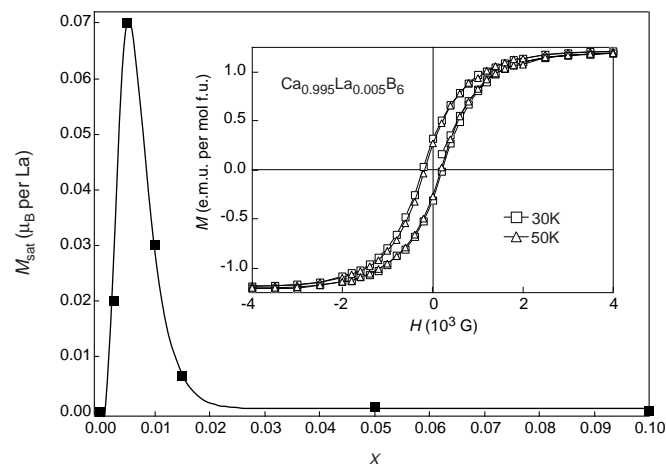
Figure 3 Saturation moment at $T = 5\,K$ per mol La as a function of La concentration in CaB$_6$. The line is a guide to the eye. Inset, hysteresis loops at 30 K and 50 K for Ca$_{0.995}$La$_{0.005}$B$_6$.

Figure 4 Magnetization of Ca$_{0.995}$La$_{0.005}$B$_6$ in a fixed applied field of 0.1 T as a function of temperature. These data were measured using a Faraday balance magnetometer.

carrier doping on the basis of the band structure of the alkaline-earth hexaborides. Calculations[10] show that the details of the overlap of valence and conduction bands at the X-point of the Brillouin zone depend sensitively on the crystallographic parameter fixing the location of the borons in the unit cell; this parameter determines the relative length of the inter- and intra-octahedral boron–boron bonds. Even small changes in this parameter in the calculations alter the behaviour from insulating to metallic. So we might expect vacancies and foreign-atom additions to alter significantly the properties of the divalent hexaborides for very small dopings, such as seen in materials with similar band structure features (for example, grey tin and bismuth).

Two suggestions for the origin of the weak ferromagnetism which we have observed are (1) ordered defect moments and (2) ferromagnetic polarization of the low-density electron gas. Because no obvious source for a strong coupling giving rise to a Curie temperature as high as $T_C = 600\,K$ presents itself, the coupling of magnetic moments localized on the La or other unspecified impurities on this scale seems rather implausible. A more likely candidate for the origin of the magnetic polarization emerges from studies of electronic correlations in the low-density electron gas, such as those of Ceperley and Alder[11]. This is a topic of theoretical speculation with a long history, going back to Block and Wigner[1]. The study of Ceperley and Alder is a $T = 0\,K$ computation, comparing unpolarized and completely polarized states of the electron gas, with ferromagnetism showing up for values of r_S of the order 80 a_B. (Here r_S is the radius of the sphere containing one conduction electron; a_B the Bohr radius.) Later calculations have lowered this value to $\sim$20 a_B (ref. 12). For $x = 0.005$, we compute $r_S = 15.0\,\text{Å} = 28.4\,a_B$, using the Bohr radius for the free electron. A recent calculation by Ortiz, Harris and Ballone[13] treating partially spin-polarized states of the low-density electron gas has, in fact, found evidence that near $r_S = 30\,a_B$ the stable state is one with ferromagnetic polarization of the order of 10%; this is essentially our experimental finding of an ordered moment of $\sim$0.07 μ_B per carrier at $x = 0.005$. The natural energy scale here is the Fermi energy, E_F; for free electrons we have $E_F = 0.062\,eV = 720\,K$ for $x = 0.005$ in CaB$_6$, of the order of the observed Curie temperature.

The ferromagnetic ground state of a dilute, three-dimensional electron gas has not previously been reported experimentally. But such a ground state seems to provide a possible description of the weak ferromagnetism reported here, although the temperature scale of the phenomenon is unexpected. Detailed calculations appropriate to the lattice case at finite temperature are clearly needed, as
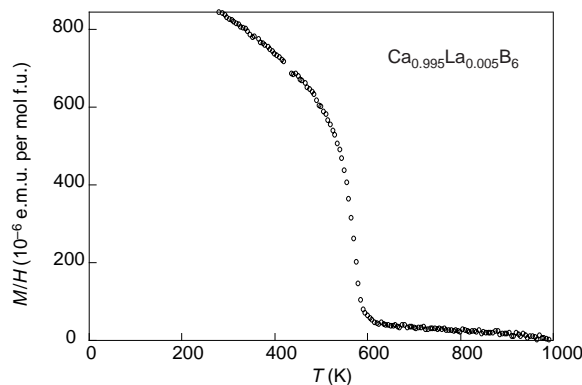
is much further experimental elaboration of the details of this ferromagnetism. □

1. Herring, C. *Magnetism* Vol. IV (eds Rado, G. T. & Suhl, H.) Ch. 2 (Academic, New York, 1966).
2. Schmidt, P. H. *et al.* Anisotropy of thermionic electron emission values for LaB$_6$ single-crystal emitter cathodes. *Appl. Phys. Lett.* **29,** 400–410 (1976).
3. Lafferty, J. M. *J. Appl. Phys.* **22,** 299–301 (1951).
4. Erkelens, W. A. C. *et al.* Neutron scattering study of the antiferroquadrupolar ordering in CeB$_6$ and Ce$_{0.75}$La$_{0.25}$B$_6$. *J. Magn. Magnet Mater.* **63/64,** 61–63 (1987).
5. Nyhus, P., Cooper, S. L., Fisk, Z. & Sarrao, J. L. Low-energy excitations of the correlation-tap insulator SmB$_6$. *Phys. Rev. B* **55,** 12488–12496 (1997).
6. Süllow, S. *et al.* Structure and magnetic order of EuB$_6$. *Phys. Rev. B* **57,** 5860–5869 (1998).
7. Degiorgi, L., Felder, E., Ott, H. R., Sarrao, J. L. & Fisk, Z. Low-temperature anomalies and ferromagnetism in EuB$_6$. *Phys. Rev. Lett.* **79,** 5134–5137 (1997).
8. Longuet-Higgins, H. C. & Roberts, M. de V. The electronic structure of the borides MB$_6$. *Proc. R. Soc. Lond. A* **224,** 336–347 (1954).
9. Ott, H. R. *et al.* Structure and electronic properties of SrB$_6$. *Z. Phys. B* **102,** 337–345 (1997).
10. Massida, S., Continenza, A., de Pascale, T. M. & Monnier, R. Z. Electronic structure of divalent hexaborides. *Z. Phys. B* **102,** 83–89 (1997).
11. Ceperley, D. M. & Alder, B. J. Ground state of the electron gas by a stochastic method. *Phys. Rev. Lett.* **45,** 566–569 (1980).
12. Alder, B. J., Ceperley, D. M. & Pollock, E. L. *Int. J. Quantum Chem. Symp.* **16,** 49–61 (1982).
13. Ortiz, G., Harris, M. & Ballone, P. cond-mat/9810126.

Improved quantum efficiency for electroluminescence in semiconducting polymers

Yong Cao, Ian D. Parker, Gang Yu, Chi Zhang & Alan J. Heeger

UNIAX Corporation, 6780 Cortona Drive, Santa Barbara, California 93117-3022, USA

Some conjugated polymers have luminescence properties that are potentially useful for applications such as light-emitting diodes, whose performance is ultimately limited by the maximum quantum efficiency theoretically attainable for electroluminescence[1,2]. If the lowest-energy excited states are strongly bound excitons (electron–hole pairs in singlet or triplet spin states), this theoretical upper limit is only 25% of the corresponding quantum